

# SACS FINAL REPORT



**Grant Agreement Number:** 3110651

**Project Acronym:** SACS

**Project Title:** Self-Assembly in Confined Space

**Funding Scheme:** FP7

**Period covered:** from 1<sup>st</sup> November 2013 to 31<sup>st</sup> October 2016

**Affiliation Project Coordinator:** Prof. Johan Hofkens, Chemistry Department, KULeuven.

**Tel.:** +32 16 32 78 04

**E-mail:** [johan.hofkens@kuleuven.be](mailto:johan.hofkens@kuleuven.be)

## Final Publishable Summary Report (1p)

Within the SACS project the researchers focused on the formation of functional structures with novel, unique properties, and this through the **self-assembly of small (sub-)nanometer-sized building blocks in restricted or controlled space** and on the formation of assemblies with strictly controlled geometries, size and shape and outstanding properties. Within this diverse concept, the synthesis focused on materials with specified functionalities such as exceptional optical properties, improved electrical conductivity and high catalytic activity. The supramolecular (hybrid) materials developed during this project had a rather diverse scope, narrowed down to three different main applications, namely innovative new phosphors, new efficient conductive materials for displays and catalytic materials. Moreover, extensive cross-pollination between the partners has resulted in materials with different functionalities and applications, beyond those envisioned in the original project description.

The emissive materials that have been developed throughout the project were based on the confinement of small metal clusters self-assembled and confined inside porous host materials, such as zeolite and other silica-based materials. The main focus of this sub-project was on the development of luminescent Ag clusters and alternative metals confined inside zeolite and MOF materials, which were synthesized through either ion-exchange/activation, sublimation or impregnation method. The samples produced within this part show emission colors spanning the whole visible light range, and exhibit high quantum yields, almost reaching unity. Within this project, the materials have been the subject of two development tracks, namely application in fluorescent lamps and LEDs, thus targeting the global lighting market. This has successfully led to the production of several lamp prototypes, which have been optimized throughout the project.

Within the SACS project, the assembly in confined space concept has been used to design and prepare novel conductive and electrochromic materials. Here, highly promising results have been obtained, as the consortium was able to identify several new materials that outperform the state of the art. The SACS materials bring along a dramatic increase of cycling speed and overall performance, when incorporated in prototype electrochromic displays. As such, we look towards further commercial development of the materials.

In its third objective, the SACS consortium aimed for catalytic applications of the nano-assembled materials. Among the envisioned applications, sustainable chemical production and clean energy production, in a.o. hydrogen conversion reactions. Several uses have been demonstrated at the laboratory scale, with attention for recyclability and scale-up potential. As key results, some of the catalytic materials outperformed the commercial standards, and hence they will be the subject of further development in collaboration with industrial partners.

To conclude, the SACS project was able to successfully investigate novel and exciting materials based on its overarching scientific concept, and develop the material into prototypes of industrial relevance. In a proliferative communication pipeline, these results have been disseminated to the scientific and general audience, in the form of no less than 44 publications and over 127 disseminations. Finally, the SACS consortium continues to push towards commercial development of its products, striving to meet the societal benefits envisioned.

## Summary description of the project context and the main objectives (4P)

The molecular-scale organisation strongly influences the electronic and chemical properties of chemical assemblies. For example application of organic and metal-complex luminophores, especially those with long wavelength absorption bands (such as organic NIR emitters), is limited by their susceptibility to chemical and photochemical degradation, their tendency to aggregate in solution, which induces multichromophoric interactions and dramatic alteration of the colour quality and the intensity of the emission signal. Similar problems relate to efficient catalysed reactions which are often restricted by low stability of the catalyst under working conditions, by toxicity, and by difficulties to precisely control and manipulate the structural organization of the catalyst at the molecular level.

As a consequence, the SACS project aims to **explore alternative routes to develop highly performing materials by exploiting molecular self-assembly**. Uniquely, this project envisions the use of a nanostructured host to control and guide the supramolecular chemistry and to ensure “electronic or structural insulation”. Next to the use of inert hosts, active hosts that are able of participating in light collection and charge transfer will be explored. This proposal combines the design, development and investigation of different families of self-assembled materials in confined spaces to obtain enhanced stabilities, new structures, emerging properties, and different processability.

Although there are currently no established mass production techniques, the non-covalent encapsulation and hierarchical organization approach offers a highly convergent protocol for the preparation of such molecular assembled hybrid materials based on: 1) Encapsulation of luminescent, chromogenic molecules or metal clusters in inert porous materials, 2) Assembly of molecules in photo- and electroactive porous frameworks, 3) Assembly of molecules on or into carbon nanotubes for the production of very efficient catalysts or new conductive materials. In the next step, these self-assembled systems will be integrated in real devices, for example via spincoating or ink-jet printing or more challenging via generating organized layers by simple self-assembly on pre-patterned substrates.

For all of these processes scaling up and low cost processability are crucial factors. Industrial partners will facilitate the generation of prototype devices such as light emitting diodes or lamps, electrochromic devices/displays and performant (photo)catalytic materials. The research is highly innovative because it introduces new approaches in material and nanoscience: 1. New techniques for obtaining self-generated ordered structures. 2. New synthetic approaches to tailor molecules, macromolecules, and hybrid nanomaterials suitable for hierarchical organization at the nanoscale. 3. Manipulation of nano-organized species by self-organization at a micrometric scale. 4. Development of novel porous and catalytic systems.

The combined expertise of the high level participating groups (the consortium hosts 2 starting and 3 advanced ERC grant awardees) contains all the necessary core competences for such studies: solid state chemistry, as well as synthetic methods from solution, will be key tools for the synthesis of novel assemblies. Hybrids of inorganic materials with organic materials will be prepared. Characterization methods comprising (basic) physical methods (e.g. X-ray diffraction, SAXS, NMR, high-resolution electron microscopy) and chemical / analytical methods (including reactivity and catalytic activities) as well as dedicated methods in the context of luminescence (e.g. time-resolved fluorescence and phosphorescence, determination of quantum yields, high resolution microscopy), will be used to

assess the structure-activity relationship. Finally, the validity of the approach will be checked by the industrial partners through the construction of prototype devices.

In more details, rare-earth based phosphors are commonly used for application as phosphors in lighting applications (Yen 2007), since these are the only commercially viable materials that are sufficiently photostable upon UV or blue excitation. These materials have light conversion efficiencies up to 80 and even 95%, reached after more than half a century of phosphor optimization. Alternative materials with promising spectral characteristics for replacement of rare-earth based phosphors, such as quantum dots based on zinc and cadmium selenides, have been developed (Yoffe 2001). However, these materials are often highly toxic and extremely expensive, and can therefore be excluded as commercially viable alternative.

Luminescence from small silver clusters, comprising just a few atoms, has been described in literature, and originates from the electronic structure that, in contrast to bulk metal, consists of discrete energy levels, where cluster size, geometry and charge determine the emission color. Recently, confinement strategies have been used to embed metal clusters in inorganic solid matrices. In particular, the molecule sized cages of zeolites are perfectly suited to accommodate oligoatomic metal clusters, since the cation exchange capacity of the zeolite framework facilitates the uptake of silver ion precursors within their pores and cages. In the proper conditions, luminescent silver species can be formed in LTA and FAU-type zeolites, by calcination of silver-exchanged zeolites. While for the LTA samples, emission quantum yields ranging from 1 to 20% have been measured, the brightest powders, with quantum yields exceeding 70% can be obtained for silver clusters in faujasite zeolites. However, this emission quantum yield was found to be highly dependent on the exact degree of hydration of the zeolites. Contact with ambient air in most cases results in a quick decrease of the luminescence. Under the proper conditions, these new materials thus approach the light conversion efficiency of rare-earth based phosphors. Within the project, these materials will be meticulously characterized and optimized for lighting use. The concept will be extended to metal-organic frameworks (MOF's), as complementary to the zeolites.

The concept of luminescent silver nanoclusters stabilized by zeolite frameworks has been extended to other metals such as copper. They are prepared in a two-step process involving first an ion exchange of the zeolites with  $\text{Cu}^{2+}$  followed by reduction by either a chemical agent (Zahmakiron 2010) or  $\gamma$ -radiation (Kecht 2006). Up to now, copper clusters in mesoporous materials have been only studied for catalytic applications while their luminescence behavior has not yet been investigated. We will thus explore the successful protocols developed for Ag-zeolite emitters also for the Cu-zeolite phosphors in this project.

The most important parameter for a phosphor material is its luminescence quantum yield (QY), i.e. which fraction of absorbed photons are converted into emitted photons of longer wavelength. Aside from the quantum yield, the shape and position of the emission spectrum is important, as it defines the color rendering index (Ra). In general, the broader the emission spectrum, the higher the color rendering index (and thus the better the experienced light quality). Unraveling the nature and organization of host species in porous materials is a challenging task. Using advanced aberration corrected transmission electron microscopy, enabling the direct observation of small silver clusters inside the zeolite host (Mayoral 2011), or by time-correlated single photon timing experiments, this project will study the most **promising phosphors in order to get insight into their structure-**

**functionality relationship.** Finally, catalytic experiments will be conducted to further valorize the Ag containing materials.

Luminescent complexes based on Cu(I) have recently attracted a lot of interest due their interesting photophysical properties (Armaroli 2007, Scaltrito 2000 and McMillin 1998) and their low cost and relatively environmentally friendliness. Hence, we intend to **explore different copper complexes in constrained space**, i.e. built in the pores of zeolites and mesoporous materials in order to stabilize their structures with respect to their coordination geometry, and even produce species which would not be stable in any other condition.

In addition, because of their negative charge, zeolites could be used for electrostatic encapsulation of cationic chromogenic compounds, such as electrochromic bipyrylium and viologen derivatives. Using the expertise of the Ynvisible company, the prepared electrochromic materials will be assembled into electrochromic cells and adequately characterized in terms of coloration efficiency, contrast and cyclability.

The formation of **metal rods/wires within the MOFs and porous materials** can also been foreseen. The seeded growth from supported nanoparticle seeds will be adapted from previous work and the resulting nanorods can be used as SERS enhancers or to enhance the luminescence of chromophore centers in doped MOFs, as recently demonstrated for quantum dots (Ma 2011), resulting in novel, highly emissive materials

Thirdly, the SACS project aims to prepare hierarchically-structured CNT-based materials in which organic or inorganic molecular guests are encapsulated inside the tubular hollow cavity that is exohedrally modified with covalent or non-covalent peripheral groups. Composites of CNTs with catalytic metals and/or metal oxides (e.g.  $\text{TiO}_2$ ,  $\text{CeO}_2$ ,  $\text{ZrO}_2$ ) have been the subject of many catalytic studies, and activity enhancements have been reported when compared to the same metal/oxide combinations without the tubes, likely for geometrical/morphological or electronic reasons (Woan 2009, Toma 2010). The SACS research will **uncover synthetic pathways to such functional materials while maintaining full control over their structure**, thus creating well defined multifunctional hybrid materials.

For example, in specific cases, it may be desired to fill the MWCNT with  $\text{Fe}_3\text{O}_4$  magnetic particles, which will enable to have a local heating effect for certain reactions, or which will facilitate magnetic recuperation of the catalyst particles in heterogeneously catalyzed liquid phase reactions.

As a first demonstration of the benefits of such catalyst design, we will study the water-gas shift reaction (WGSR) and the preferential oxidation of CO (PROX) in a reducing  $\text{H}_2$  atmosphere. Both reactions are highly relevant to produce high purity  $\text{H}_2$ , which is as much as possible free of CO that would inhibit the fuel cell electrocatalysts. For the WGSR, it is expected that the direct contact between the metal particles and the CNTs would prevent catalyst deactivation during reaction carried out under reducing conditions where the metal is electronically deactivated by the reduced support, as is the case in the WGSR using conventional Pd/ $\text{CeO}_2$ . As a second energy-related application, we will study the electro-oxidation of alcohols, as encountered in direct alcohol fuel cells, using the modified CNTs as anode material.

Within SACS, **prototypes based on the newly developed self-assembled building blocks will be generated** in close cooperation with the industrial partners. A prototype lamp or LED with the newly assembled phosphors and emissive CNTs will be developed where suspension preparation and coating will be done on lab scale, together with industrial partner Philips. Based on the lamp results (output, CPU, degradation) several test-loops will take place, until a good performing product can be achieved.

Accelerated lifetime testing Lifetime is one of the key performance parameters of light emitting devices. It is commonly defined as the time for luminescence to decrease to half of its initial value. In a more general context, lifetime may be defined as the loss of functionality of the device, determined by changes in emission uniformity, photobleaching of the emitters, temperature, emission color, etc. These types of measurements have been used recently to test the operation of light emitting diodes and we intend to use a similar approach in order to evaluate the photodegradation of our materials.

Thirdly, the materials will be used in electrochromic devices. In such devices, the light transmission properties and, therefore, the color exhibited, can be changed in a controlled and reversible manner (based on redox reactions) when an electric current flows through the device. The most typical color exhibited by electrochromic displays is blue, but there is a market need for other colors. On the other hand, many electrochromic compounds are prone to degradation due to electrochemical and chemical reactions and there is a need for stable electrochromic compounds, which can be formulated and printed. This particular point joins the need for replacing indium-tin oxide (ITO), as the conductive material layer in the device, as the main technical challenges in the field of electrochromic devices. The new self-assembled encapsulated electrochromic SACS materials and conductive materials comprising carbon nanotubes will be critical for addressing these challenges and for progressing beyond the current state of the art. In the SACS project, Ynvisible (P8) will contribute to the exploitation and validation, at a preindustrial level (prototyping), of the newly developed electrochromic and conductive materials, as components of electrochromic devices. Ynvisible is bringing in expertise in: ink formulation (electrochromics formulation and conductive ink formulation), printing/deposition, device assembly and characterization, design and electronics. Proof of concept, prototypes, and demonstrators will be prepared by Ynvisible having different configurations, but typically in a multilayer structure format.

## Main S&T results/foreground (25P)

### Description of main S&T results/foreground

#### WP1

Work package 1 focused on the formation of small oligoatomic metal clusters confined inside porous materials, in order to synthesize materials with remarkable luminescent and catalytic properties.

In a first part, silver clusters were confined inside zeolite scaffolds, by exchanging Ag-ions and subsequently activating them through methods such as heat-treatment. Two types of zeolites have been used for the self-assembly and confinement of these Ag clusters, namely faujasite-type (FAU) and Linde type A (LTA) zeolites. Both zeolites have high cation exchange properties and consist of sodalite cages as secondary building blocks. These sodalite cages can be used for the ship-in-a-bottle confinement of the luminescent Ag cluster. The materials prepared showed very unique luminescent properties, with emission colors spanning the whole visible spectrum. A portfolio of these materials has been studied; and the best candidates are depicted in table 1. It should be noted that the lead candidates for further development are currently approaching the commercial standards regarding performance.

**Table 1.** Composition and optical properties of commercial and Ag-zeolite based phosphors.

Sample	Excitation Max (nm)	Emission Max (nm)	Color	QY (%)
<b>Commercial phosphors</b>				
Phosphor_red[Y <sub>2</sub> O <sub>3</sub> :Eu]	258	611	Red	91
BAM_green [BaAl <sub>12</sub> O <sub>19</sub> :Mn <sup>2+</sup> ]	315	515	Green	89
BAM_blue [MgBaAl <sub>10</sub> O <sub>17</sub> :Eu]	315	450	Blue	94
<b>Ag-zeolite phosphors</b>				
Na-LTA_1	260	440	Blue	21
Na-LTA_2	280	540	Green	62
Na-LTA_3	280	690	Red	41
Li-LTA_1	280	560	Yellow	62
Li-LTA_2	350	545	Green	83
K-LTA_1	330	540	Green	30
K-LTA_2	280	490	Green	59
Na-X_1	330	565	Yellow	43
NaY_1	310	540	Green	88
NaY_2	310	540	Green	97
NaY_3	310	485	Blue	89
NaY_4	260	485	Blue	91

A thorough material characterization effort was launched within the project, to improve the understanding of the processes and materials at hand, and to support further optimization. As such, when studying the LTA zeolites two observations can be made: first of all, the differences in emission color are larger compared to the FAU-type zeolites; secondly, it can also be seen that the EQE of the Li exchanged LTA zeolite, having Li as counterbalancing ions next to Ag, are remarkably higher than the other LTA-type zeolites reaching values up to 83 %.

From these results of the FAU-type zeolites it can be seen that several Ag-FAUY zeolite phosphors display very high external quantum efficiencies (EQEs), with one sample reaching an EQE of almost

unity (97 %, this sample was prepared through a collaboration between KU Leuven and the group of P. Samori at UniSTRA). FAUX zeolites on the other hand reach maximal EQE of 43 %.

These FAU samples were also visualized using HAADF-STEM to determine the cluster structure in these samples (Figure 1), and this in combination with XRD analysis. These experiments were conducted in collaboration with the EMAT centre, at the University of Antwerp. From these results, it was shown that inside FAUY a linear  $\text{Ag}_3$  cluster was formed, while in the FAUX sample this linear  $\text{Ag}_3$ -cluster is coordinated with a silver-ion inside the sodalite cage. This weak coordination is related to the shift from green to yellow emission for the FAUY and FAUX sample, respectively.

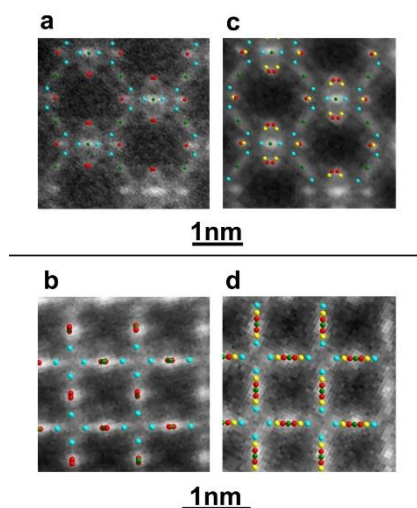


**Figure 1.** a) and c) Overlay between the averaged HAADF-STEM images and the models obtained from XRD along the  $[110]$  zone axis for both the cation-exchanged (a) and heat-treated (c) forms of Ag-FAUX. b) and d) Overlay between the averaged HAADF-STEM images and the models obtained from XRD along the  $[100]$  zone axis for both the cation-exchanged (b) and heat-treated (d) forms of Ag-FAUX.

To further our understanding of the origin of these exceptional PLQYs in FAU zeolites, characterization of the clusters structure which pursued, and this using EXAFS in collaboration with the Laboratory of solid-state physics and magnetism (KU Leuven). It emerged from our data that, in FAUY[ $\text{Ag}_{0.5}$ ], about 67% of silver atoms ( $\text{Ag}_c$ ) form  $\text{Ag}_4$  clusters inside the sodalite cages in which each Ag atom is bonded to 2.2 water molecules with the remaining (about 33%) silver atoms being non-cluster-forming  $\text{Ag}_R$  (about 18%) and  $\text{Ag}_P$  (about 15%) cations. Similar EXAFS analysis of the fully Ag-exchanged sample FAUY[ $\text{Ag}_{6.5}$ ] also have revealed  $\text{Ag}_4$  cluster structure, but with slightly fewer silver atoms involved in cluster formation (about 62%).

This different trend in PLQY for FAUX is of special interest. The absence of new peaks in the excitation–emission spectra with increasing silver loading indicates that the nuclearity of luminescent clusters formed in FAUX zeolites is not dependent on silver loading; a similar observation can be made for FAUY. We therefore considered that luminescent cluster formation must be hindered at low silver loading in FAUX. This is supported by EXAFS analysis (Figure 1) that shows that Ag clusters have a nuclearity of about 4 in all our FAUX zeolites, but a significantly lower proportion of silver atoms form clusters at low silver loadings than at high loadings (about 57% in FAUX[ $\text{Ag}_1$ ] compared with about 73% in FAUX[ $\text{Ag}_3$ ]). This is the opposite trend to FAUY and consistent with the drop-off in PLQY at low silver loadings in FAUX, although not enough by itself to explain such low efficiencies. In fact,  $\text{Na}^+$  ions are more mobile than  $\text{Ag}^+$  ions in FAUX, but the opposite is true for FAUY. We speculated that the reason for this counter-intuitive trend in ionic conduction is the trade-off between the Coulombic framework–cation interaction, which decreases for larger ionic radii, and cation–cation repulsion, which increases



with ionic radius and is more prominent in FAUX zeolites than FAUY owing to the higher cation density. Cation–cation repulsion should decrease silver ion mobility with increasing silver content, which may be responsible for the greater degree of disorder in clusters in FAUY at high silver loading along with static effects such as poorer charge balance in the zeolite. Closer analysis of the EXAFS signal of FAUX[Ag<sub>1</sub>] revealed a sodium shell around the silver clusters that could not be detected in FAUY. This strongly suggests that sodium ions, which are more concentrated and more mobile in FAUX compared with FAUY, are playing a key role. Owing to their high mobility relative to Ag<sup>+</sup> in FAUX, they are able to move to sites inside the sodalite cages, interfering with silver cluster formation and affecting the electronic/geometric structure of silver clusters that do form. EXAFS also revealed that the sodium reduces the amount of water coordinated to the cluster, which may also reduce PLQY. This highlights another important aspect to the role played by counter-ions in luminescent cluster formation.

LTA in its lithium form (LTA[Li], 33 % cation replacement) was employed to fabricate a novel class of Ag-zeolite phosphors with remarkable luminescence performance. By partially replacing sodium with lithium ions as counter-balancing agents in the LTA zeolite scaffold, a new type of luminescent silver zeolite composites in which, for the first time, the presence of more than one emitting species, depending on the water content, was synthesized. These new type of phosphors possess high external quantum efficiencies (up to 62 %) and display an emission that dynamically change colors with respect to their hydration level (Figure 2).

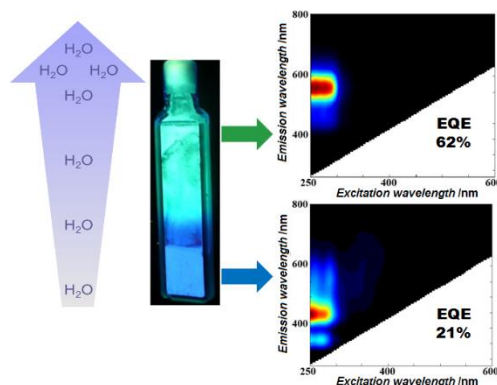


**Figure 2.** Water dependence of the emission color observed in LTA(Li)-Ag<sub>1</sub> composites. In fully hydrated samples (19 % water content) a green emission was found, whereas in partially hydrated samples (2 % water content) blue emission was recorded.

The dependency on the hydration could be explained by studying the structure of the luminescent Ag cluster using EXAFS at the ESRF in Grenoble, France. This research shows a change in the clusters nuclearity, from around 4 in the hydrated state down to 3 Ag atoms in the partially dehydrated samples.

In a second part of the study, alternative metals to silver were investigated for use in the synthesis of luminescent clusters confined inside zeolite templates. The tested metals were selected following two criteria. The first one is based on literature reports (Claffy E.W., Preliminary Observations on the Luminescence Activation of Zeolite Minerals by Base Exchange, 1951), which describes cathodoluminescence in Au, Mn, and Pb exchanged natural zeolites. The second criteria is based on availability, toxicity and price of the metal precursors.

The exchange and activation of Mn<sup>2+</sup> resulted in the synthesis of weakly luminescent samples. After analysis of their luminescent properties, a wide range of excitation and emission wavelengths and an EQE of about 5% was observed. The luminescent is thus probably coming from multiple Mn species which are confined inside the zeolite structure. These non-selective formation of emissive Mn species

makes it very difficult to produce Mn-zeolite phosphors with very high quantum efficiencies and thus the research moved on to other metal precursors.

Another interesting metal precursor is lead, LTA zeolites exchanged with  $Pb^{2+}$  show very remarkable luminescence properties after heat-treatment and dehydration. From this research it was found that the sample with a Pb content of 3 wt% and treated at 200 °C, displays the formation of luminescent Pb species with a quantum efficiency of 70 % and an excitation and emission maximum of 250 and 390 nm, respectively (Figure 3)

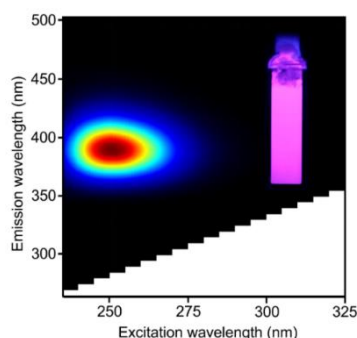


**Figure 3.** Two-dimensional (2D) excitation/emission plot of the dehydrated  $Pb_{0.25}$ -LTA sample, the inset displays a picture of the sample in a cuvette under 254 nm-illumination.

Zinc and copper are the metals which were found to comply with these conditions. The synthesis procedure of these metal cluster formation is similar to the one followed for the silver clusters confined in zeolites. Preliminary tests revealed that heat-treated Zn-LTA zeolites possess interesting luminescence properties. The samples showed a broad orange emission peak when excited at 250 nm and quantum efficiencies up to 25 %. The tests carried out using Cu as metal precursor will be further discussed in WP2

In a third part the fabrication of phosphor materials was based on the confinement of Ag clusters confined inside MOF materials. One of the most interesting materials from a screening of different MOF materials is bio-MOF-1 (4,4'-biphenyldicarboxylate; 4,4'-BPDC). Upon exchanging Ag in to bio-MOF-1 different mild reducing exchange solvent were optimized, by varying the water/ethanol-ratio, to have an in situ formation of the luminescent Ag species, which were observed at intermediate EtOH- $H_2O$  ratios (Figure 4). This new luminescent feature has an emission at 485 nm quantum yields reaching 18.6% (i.e. < 20%). These changes in luminescence were also coupled to changes in the crystal morphologies from bio-MOF-1 to MOF-69A, determined by SEM and PXRD using Pawley refinement.

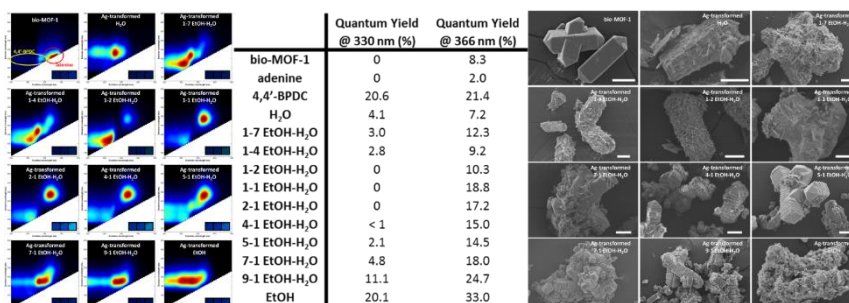


**Figure 4.** (A) Luminescent study of Ag-induced structural transformation of bio-MOF-1, (B) quantum yields at 330 nm and 366 nm, (C) SEM images (scale bar 10  $\mu m$ ).

In a final section, MOF structure UiO-66 and porous  $SiO_2$  and  $Al_2O_3$  were impregnated with Ag Nanoparticles, which were subsequently tested as catalyst in the chemoselective hydrogenation of

cinnamaldehyde (CALD). Catalytic activity of UiO-66 supported silver is clearly visible; in contrast to the thermodynamically favored C=C hydrogenation, cinnamyl alcohol (CALH) is the preferentially formed product with a selectivity of  $66 \pm 3 \%$  (Table 2, entry 1). Reference Ag/SiO<sub>2</sub> and Ag/Al<sub>2</sub>O<sub>3</sub> catalysts with similar Ag-loadings were used under the same reaction conditions (Table 2, entry 5-6). The Ag/SiO<sub>2</sub> powder shows a comparable reaction selectivity ( $71 \pm 3 \%$ ), however with a slightly higher hydrogenation rate (TOF of  $6.1 \pm 0.1$  mol CALH/mol Ag/h). On the other hand, strongly reduced CALH selectivity of  $47 \pm 5 \%$  was obtained with Ag/Al<sub>2</sub>O<sub>3</sub>. This is most probably related to the formation of larger Ag nanoparticles as seen on powder XRD of this black powder. Thus, the choice of the support has an important influence on the formation and stabilization of the Ag nanoparticles and the resulting catalytic properties. To confirm that the observed catalytic activity can solely be attributed to the Ag nanoparticles, the reaction was also performed with pure UiO-66. As can be seen in Table 2 (entry 4) no significant conversion of CALD was detected in this blank reaction after 6 h.

**Table 2.** Conversion and selectivity in the reduction of cinnamaldehyde (CALD) in *N,N*-dimethylacetamide, catalysed by UiO-66, Ag/UiO-66 and a Ag/SiO<sub>2</sub> reference catalyst.

Entry	Catalyst	H <sub>2</sub> (bar)	Wt% Ag <sup>(a)</sup>	X (%)	TOF <sup>(b)</sup>	S <sub>CALH</sub> (%)	S <sub>HCAL</sub> (%)	S <sub>HCALH</sub> (%)
1	Ag/UiO-66	30	14	82	3.3	66	30	2
2	Ag/UiO-66	40	10	64	3.5	69	29	1
3	Ag/UiO-66	50	10	>99	5.5	66	27	6
4	UiO-66	30	0	<1	/	/	/	/
5 <sup>(c)</sup>	Ag/SiO <sub>2</sub>	30	13	90	6.1	71	28	1
6	Ag/Al <sub>2</sub> O <sub>3</sub>	50	13	96	2.9	47	36	18

CALD= cinnamaldehyde, CALH= cinnamyl alcohol, HCAL= hydrocinnamaldehyde, HCALH= hydrocinnamyl alcohol ; Reaction conditions: CALD (1.15 mmol), *n*-tetradecane (0.95 mmol), solvent *N,N*-DMA (3.3 mL), 25 mg catalyst, 140 °C, 6 h, 500 rpm. <sup>a)</sup>determined via ICP-AES <sup>(b)</sup>mol CALH per mol Ag per h <sup>(c)</sup>4 h

## WP2

This work package focused on the formation of new hybrid materials based on Copper complexes as well as photo- and electrochromic molecules stabilized inside porous hosts.

A novel way to synthesize luminescence Copper(I) clusters into porous materials was developed in the first part of this work package. Different techniques have been evaluated for this encapsulation, such as sublimation of CuI and Cu-complexes inside zeolite scaffolds and the incorporation of Cu-complexes into mesoporous silica or the synthesis of mixed crystals.

For the incorporation of copper iodide into zeolite Y, both materials were placed under vacuum ( $10^{-6}$  mbar) then heated up to 250°C in order to sublime the CuI in the pores of zeolites. The material, CuI@Zeolite, exhibits similar photophysical properties than CuI clusters crystals, meaning we created CuI cluster inside the pores of zeolite by a simple sublimation. As the Cu(I) clusters may be sensitive to oxygen, it can be useful to stabilize it with ligands, such as triphenylphosphine and Pyridine. The binding of Pyridine to the cluster induces a change in the emission wavelength to  $\lambda_{\max}^{\text{em}}=575\text{nm}$  with an increase of the PLQY up to 34%. It is noteworthy that the clusters also exhibit thermochromic effect (Figure 5).

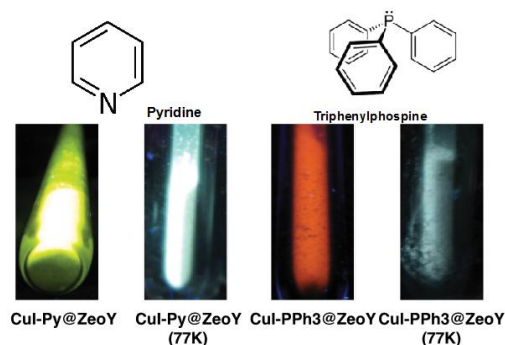


**Figure 5.** Change in the emission color upon freezing the solution (thermochromism) of clusters inside zeolites.

A second strategy to obtain different emissive Cu(I) compounds is the formation of Cu(I) halides inside mesoporous materials. The resulted copper cluster inside porous zeolites, shows deep red emission centered with a wavelength of around 700 nm. The photoluminescence quantum yield of the cluster is about 10% with tunable colors and emission quantum yields up to 34% by adding an organic ligand after the formation of copper cluster (Figure 6).

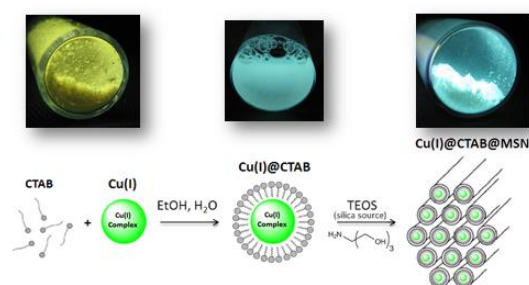
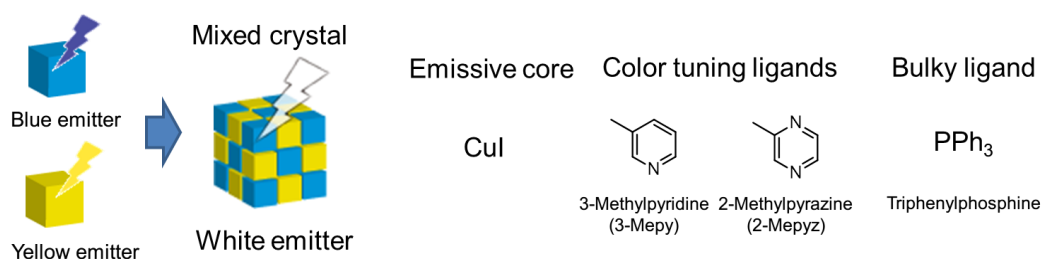


**Figure 6.** Synthesis of the copper(I) based luminescent material

In the final strategy, mixed crystals are synthesized to make Cu-based phosphors. Mixed crystals are species consisting of a solid solution of two or more distinct compounds. If mixed crystals are composed of two or more emitters, each one showing a different emission colour (e.g. blue and yellow or blue, green and red), the mixed crystals are expected to exhibit white emission (Figure 7). The Cu(I)-halide complexes with N-heteroaromatic ligands have the advantage that their emission colours can be changed by minimal structure change, i.e. only replacement of ligands. By synthesizing mixed crystal based on 3-methylpyridine and 2-methylpyrazine ligand, we are able to obtain white light emitters with PLQY reaching up to 83% (Table 3).



**Scheme 7.** Concept of the mixed crystals formation and formulas of the ligands employed

**Table 3.** Photophysical properties of the different mixed crystals

Composition ratio	$\lambda_{\max}^{\text{em}}$	$\Phi_{\text{em}}$	CIE
(3-Mepy : 2-Mepyz)	(nm)	%	(x, y)
100:0	481	83	(0.20, 0.29)
97:3	505	79	(0.28, 0.38)
95:5	528	70	(0.35, 0.52)
75:25	543	75	(0.37, 0.52)
0:100	546	65	(0.40, 0.54)

In the second part electrochromic hybrid materials were investigated, in such way they reach 5000 cycles, possess a switching time <2s and a good coloration efficiency, when assembled on an electrochromic device. In order to achieve this goal, two different strategies were pursued. FFCT-UNL developed an approach based on *Electric Assisted Self-Assembly* (EASA) method, via electrodeposition of electrochromic films. Ynvisible developed mesoporous silica and TiO<sub>2</sub> particles with electrochromic polymer for further use using standard printing techniques such as screen-printing.

The EASA method consists of the electrochemical polymerization of PEDOT from EDOT monomers on bare FTO electrodes and on template-extracted mesoporous silica films deposited by EASA on FTO electrodes. The mesoporous silica thin films have vertically-aligned pore channels of 2–3 nm in diameter, closely packed in a hexagonal arrangement. The FTO surface was present at the bottom of each pore of the mesoporous silica film and was used to electrochemically synthesize PEDOT in each of the film pores. Solid-state electrochromic devices (ECDs) were assembled with these films as displayed in Figure 8. Although this EASA method shows the production of working electrochromic devices, the goal of 5000 cycles was not reached.

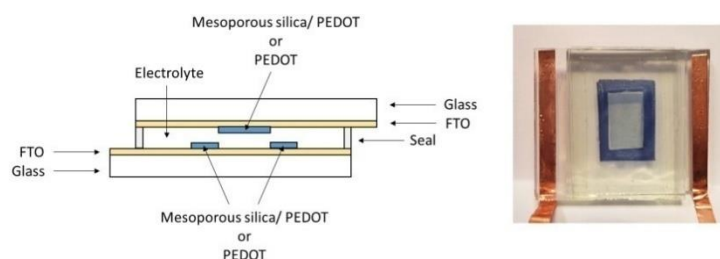


**Figure 8.** Cross-section (not to scale) of the solid-state electrochromic device architecture used in this work. Glass substrates are offset to allow attachment of conductive adhesive copper tape to the FTO electrodes for electrical contact. A photograph of the ECD is also shown.

The other procedure followed includes the deposition of the inorganic material, such as TiO<sub>2</sub>, was developed and then proceeded to the electropolymerization of the monomer. Three different monomers were used: EDOT (3,4-ethylenedioxythiophene), 3MT (3-methylthiophene) and DMT (3,4-dimethoxythiophene). With this protocol for the electrosynthesis of electrochromic hybrid materials in glass-FTO electrodes, we were able to achieve electrochromic devices that presented a cyclability over 50000 cycles for the hybrid materials *PEDOT@TiO<sub>2</sub>* and *PDMT@TiO<sub>2</sub>*, 10 times more that the milestone required. In the case of the hybrid material *P3MT@TiO<sub>2</sub>* only reached 2000 cycles due to the harsh solvent conditions. In terms of switching time all the polymers and hybrid materials presented switching times below 2 seconds. The coloration efficiency of the devices is rather good, with a slight decrease in the case of hybrid materials due to the charge consumption of the TiO<sub>2</sub> material.

In the third part photochromic materials were investigated by using two different strategies, namely by synthesizing hybrid and complete inorganic materials, since photochromic systems are frequently produced using organic compounds, of which degradation can be a strong. Production of inorganic and hybrid photochromic materials can circumvent this, since the stability of such materials is much higher.

Synthesis of inorganic photochromic materials was based on the mineral Hackmanite, which displays photochromicity and/or photoluminescence. This mineral has a sodalite composition,  $\text{Na}_8[\text{SiAlO}_4]_6\text{Cl}_2$ , and can be photochromic, where a deep pink or violet colour appears on exposure to UV radiation, due to the existence of  $\text{S}_2^{2-}$ . This effect is reversible since the energy derived from white light, in particular green light range, allows the electron to return to his original place, giving rise, once again, to a white sample.

The materials in this project were synthesized starting from commercial LTA zeolite, to which different stoichiometric amounts of  $\text{Na}_2\text{SO}_4$  and  $\text{NaCl}$  ( $\text{NaBr}$  or  $\text{NaI}$ ) were added and after a 30 min ball-milling, the mixture of powders were annealed in air for 8h at 800 °C, after which a pellet was pressed and treated in a horizontal tubular furnace for 8h at 900 °C under a reducing atmosphere (7%  $\text{H}_2$ , 93%  $\text{N}_2$  (v/v))

the synthesized materials were white as-prepared, however when exposed to 254 nm radiation for a few seconds, using a determined sulfur/chloride concentration, a pink colour appears, with a corresponding absorption centered at 530 nm and with a good colour contrast, due to the presence of  $\text{S}_2^{2-}$ . Afterwards when irradiated with a green light it turns again, instantaneously, to the original colour, figure 9.

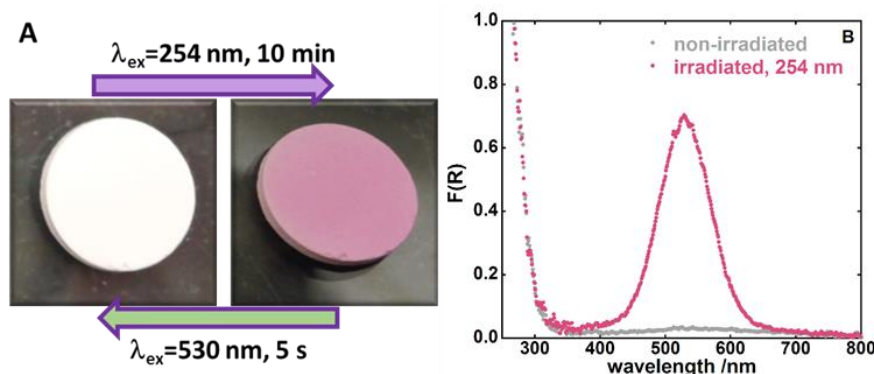


**Figure 9.** (A) Sample  $\text{Na}_8[\text{SiAlO}_4]_6\text{S}_{0.25}\text{Cl}_{1.5}$  exposed to 254 nm radiation and the reversible behaviour when exposed to a 550 nm radiation. (B) Diffuse reflectance UV-Vis absorption spectra, Kubelka-Munk, of the same sample non-irradiated and after irradiation with a 254 nm UV lamp during 10 min.

The samples show fast switching time, which is strongly depend on the intensity of the light source. Furthermore the synthesized samples are very stable, since it was possible to perform several cycles, maintaining, taking in consideration some measurement errors, the same colour intensity and it can be observed that even after more than one year, the synthesized sample is still very stable.

Changing some of the synthesis conditions of the previous mentioned samples led to the formation of luminescent  $\text{Na}_8[\text{SiAlO}_4]_6\text{S}_x\text{Cl}_{2-x}$  materials, with rather large Stokes Shifts, Quantum Yields and temperature stability. An emission band at 650nm for low sulphide contents is observed, fully consistent with  $\text{S}_2^-$  clusters as light emitting centers. For higher x values a conversion to other light emitting centers at 780nm is observed (figure 2.2.13), attributed to polysulfide clusters (presumably



$S_4^{2-}$  species). Rather large photoluminescence External Quantum Efficiencies (EQE) are observed for  $x=0.2$  (53%), but with increasing  $x$  a quenching is observed, as depicted in figure 10.

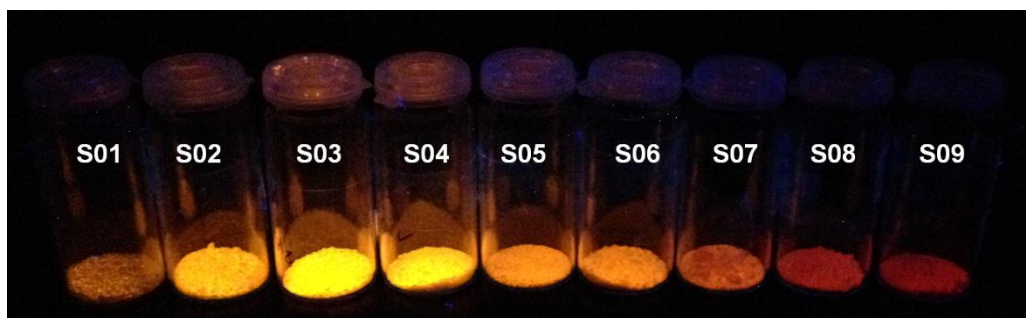


**Figure 10.** Luminescent sodalites corresponding to the stoichiometry,  $Na_8[SiAlO_4]_6S_xCl_{2-x}$ ,  $x = 0.1; 0.2; 0.3; 0.4; 0.5; 0.6; 0.7; 0.8$  and  $0.9$ , under an UV light,  $\lambda_{ex}=364$  nm.

Within this project a new hybrid photochromic mesoporous material was prepared based on flavylum guests, 3'-butoxy-7-hydroxyflavylium hydrogensulfate (FI-OH) and 3'-butoxy-7-methoxyflavylium hydrogensulfate (FI-OCH<sub>3</sub>), covalently attached to MCM-41 and SBA-15. The new hybrids show pH-dependent reflectance spectra resembling those observed in solution, but shifted to higher pH ranges, indicating a higher stability of the grafted flavylium cations.

Irradiation of these materials, equilibrated at adequate pH values where the photoisomerizable *trans*-chalcones predominate, shows formation of the respective flavylium cations, which recover back to the initial compositions upon standing in the dark. Leading to new organic-inorganic hybrids as pH-dependent photochromic materials with relatively fast kinetics for colour change (minutes under our working conditions). However, these pigments show very high degradation and only last for a few cycles.

In order to increase the stability of the photochromic contrast, halide-free pigments were synthesized, using different surfactants in which the anion was changed. The selected anions were: acetate (Ac), dicyanamide (DCA) and chloride (C), and the resulting surfactants are CTA-Ac, CTA-DCA and CTAC, respectively. CTA-DCA resulted in a very stable photochromic pigment highly resistant to photochromic stress. After 3 hours of continuous irradiation, the photochromic performance is still very close to the original within experimental error (9% of degradation).

In a final part of this work package, photoactive porous systems were produced, in which metal particles were encapsulated within a mesoporous material. These particles can be used as plasmonic enhancers of chromophore centers placed inside the pores. The research mainly focused on silica as mesoporous material and gold as metal core, and this because of their suitability for biological applications. We optimized a protocol for the coating metallic particles with mesoporous silica particles with radial channels of 2.3 nm (Figure 11 a-d). All these particles are stable in ethanol and water (after a temperature treatment) and can be dried for storage. By using these silica coated particles as seeds, and their radial silica channels as a template, we were able to grow gold wires from the gold cores (Figure 11 e-h).

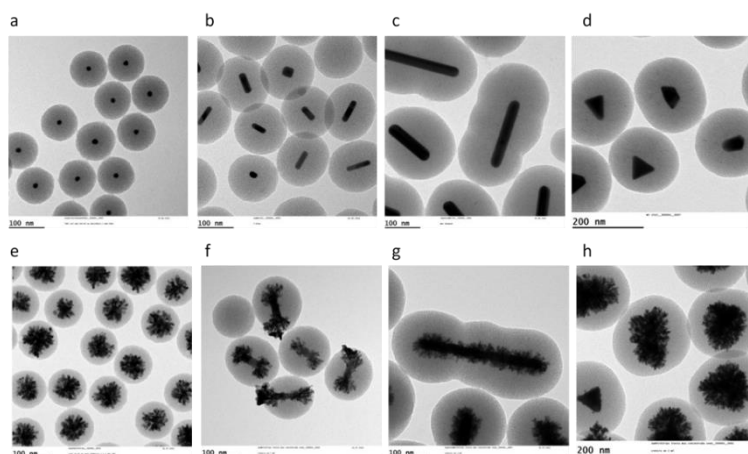


**Figure 11.** TEM images of mesoporous silica coated gold particles with different shapes(a-d) and TEM images of spiked mesoporous silica coated gold particles(e-h).

These type of materials we successfully applied in two SERS systems, namely the monitoring the dye delivery through gates and the label-free nanosensing for antibiotic detection.

### WP3

This work package focused on the advanced design and synthesis of innovative Carbon nanotube (CNT)-based materials employing Multi wall CNTs (MWCNTs) and single wall CNTs (SWCNTs) together with related nanostructures, as templates for the controlled arrangement of functional molecules. In order to produce Fe-filled MWCNTs@metal/oxide nanocomposites for heterogeneous catalysis, hierarchically-assembled Chromophore-filled CNT-based photosynthetic systems were prepared and investigated for the use of CNT frameworks as emissive, chromogenic and conductive materials.

The synthesis of Fe-filled multi-wall carbon nanotubes (Fe@MWCNTs) with high amounts of loadings in magnetic nanoparticles was achieved by *floating-catalyst chemical vapour deposition* (FC-CVD) by UNamur. Moreover, it was shown that different synthetic conditions would lead to different material properties due to the presence of different Fe loadings and Fe phases ( $\alpha$ -Fe,  $\gamma$ -Fe and Fe carbides) encapsulated inside the MWCNTs (Fe@MWCNTs). A set of four Fe@MWCNT derivatives was thus synthesized using different synthetic conditions and post-synthetic treatments, to evaluate their influence on the structure and composition of the materials (Figure 12). The four different materials were characterized by several techniques (XPS, TGA, TEM, PXRD,  $^{57}\text{Fe}$  Mossbauer, among others). In particular, their magnetic properties such as magnetic saturation ( $M_s$ ), coercivity ( $H_c$ ) and low-field magnetic susceptibilities ( $\chi$ ) were evaluated depending on the composition and treatment of the materials. A synthetic protocol for the synthesis of more complex hybrids, incorporating Pd nanoparticles embedded within the metal oxide phase, was also successfully developed and subsequently investigated as recyclable catalysts.



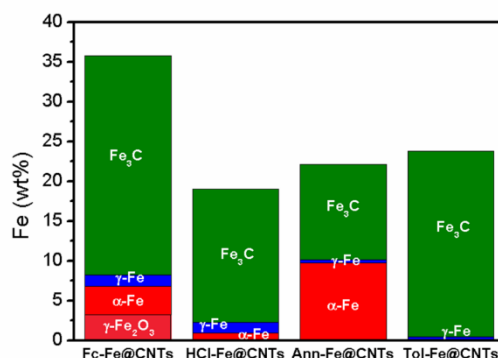


**Figure 12.** Histogram distribution of the Fe phases in the four materials as assessed by  $^{57}\text{Fe}$ -Mössbauer spectroscopy and TGA measurements under air.

In a collaboration between UCardiff and INSTM, a series of nanohybrids featuring Fe-filled carbon nanotubes covered with uniform layers of metal oxides were synthesized. The chosen metal oxides ( $\text{TiO}_2$ ,  $\text{CeO}_2$ ,  $\text{ZrO}_2$ ) are materials of catalytic interest, being employed in many systems and were prepared by employing either a sol-gel approach or a solvothermal approach. Additionally, metal oxide embedding Pd nanoparticles were also synthesized based on the preformation of core-shell precursors  $\text{Pd@MO}_x$  ( $M=\text{Ce}$ ,  $\text{Ti}$ ), followed by sol-gel step and controlled hydrolysis to produce the final hybrids. The composition of the systems was varied by changing the nominal weight percent of the MWCNTs building blocks.

The catalytic potential of the as-prepared hybrids for a number of energy-related processes of industrial relevance were subsequently screened. Additionally, we evaluated the performance in relation to specifically developed magnetic purification protocols and magnetic recycling protocols. It turned out that a general trend indicates the superiority of the magnetically purified materials as compared to materials purified by standard filtration techniques. Magnetic recyclability was also encouraging, with almost 85% of the catalysts recovered, and with retaining of activity after the first catalytic run.

$\text{Fe@MWCNTs}\cap\text{Pd@TiO}_2$  was employed in the photo reforming of methanol for the production of  $\text{H}_2$ , where it was displaying a higher activity as well as higher stability compared to filtration purified catalysts and Fe-free catalysts.

$\text{Fe@MWCNTs}\cap\text{Pd@CeO}_2$  was employed as a catalyst in the water-gas shift reaction. We used the nominal composition with 5% MWCNTs, which however turned out to be 30%wt as shown by TGA data. The activity of the better catalyst were, however, similar to those of a reference catalyst prepared using Fe-free nanotubes. However, the two catalysts showed to bear a different amount of  $\text{CeO}_2$  by TGA, so the comparison is biased towards the Fe-free catalyst.

Additionally the electrocatalytic activity of  $\text{Fe@MWCNTs}$  in oxygen reduction (ORR) and hydrogen evolution (HER) reactions at neutral pH was tested. Our conclusions are that the Fe decreases the local work function on the carbon surface due to electron transfer processes from the inner Fe particles to the graphitic shells. On the other hand, the MWCNTs mediate the electron transfer towards the reactive species and protect towards uncontrolled Fe oxidation or leaching. For ORR, we found that the benzylic acid functionalized  $\text{Fe@MWCNTs}$  exhibited the best performance, with an onset potential of  $E_{\text{onset}} = 0.02 \text{ V}$  and a sensitivity of  $8.9 \times 10^2 \mu\text{A}\cdot\text{L}\cdot\text{mg}^{-1}\cdot\text{cm}^{-2}$ . By comparison, sensitivity of the electrode modified with commercial MWCNTs was only  $3\mu\text{A}\cdot\text{L}\cdot\text{mg}^{-1}\cdot\text{cm}^{-2}$ . For the HER, the  $\text{Fe@MWCNTs}$  is also superior to commercial MWCNTs, with an overpotential of 0.8 V versus the 1.05 V of the latter.

Furthermore Cr-functionalized CNTs were used as scaffold for the preparation of new photosynthetic materials by covering them with layers of TiO<sub>2</sub>. Given the poor photocatalytic activity, some modification was also introduced in order to make the catalysts active materials for energy applications and artificial photosynthesis.

Regretfully, despite several efforts in the synthesis of the photosynthetic materials did not lead to any photocatalysed CO<sub>2</sub> reduction activity, which is an important step for future artificial photosynthesis. Evidently, the hurdles for performing CO<sub>2</sub> reduction utilizing only visible light are very high, and call for a deeper scrutiny of the photosensitizer to be used, which could be completely different and more complex than the porphyrins employed, and this should be the focus of future research.

On the other hand, very encouraging results with the electrocatalytic CO<sub>2</sub> reduction were obtained. Formate is a difficult product to obtain, and, at least in the first one hour, the SWCNHs/Pd@TiO<sub>2</sub> system shows performances that outcompete those of state-of-the-art catalysts. Current work is focused on tackling the complete elimination of the side H<sub>2</sub> evolution process.

In order to drive energy-related processes with enhanced efficiency, particularly photocatalytic processes, previous reported catalytic materials were optimized and new nanocatalysts were designed. The starting point was the assembly of three-phases nanomaterials, based on MWCNTs covered with layers of titania embedding Pd nanoparticles. This time, the materials were subjected to thermal treatments (MWCNTs/Pd@TiO<sub>2</sub>-calc), with the purpose of crystallizing TiO<sub>2</sub>, thus making it more photoactive, and simultaneously remove the organic groups, making the contact between MWCNTs and TiO<sub>2</sub> tighter (Figure 13).

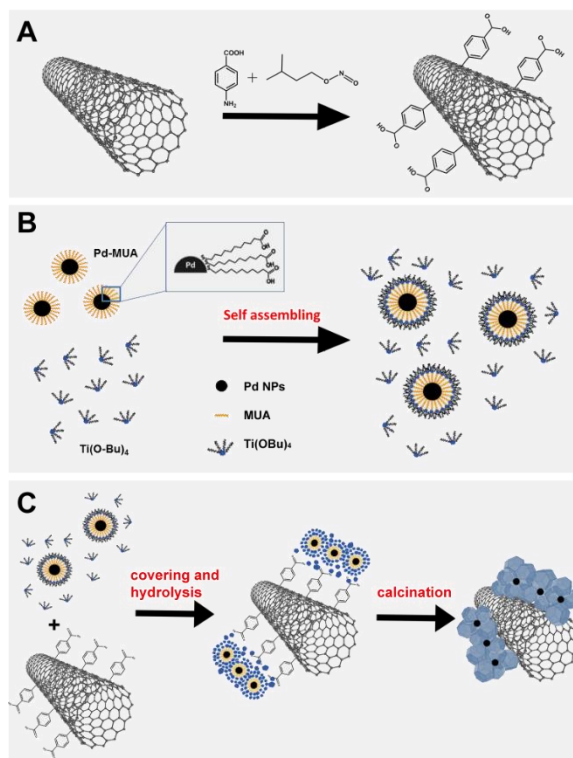


**Figure 13.** Complete synthetic scheme to access the final nanohybrid MWCNTs/Pd@TiO<sub>2</sub>-calc

The photocatalytic activity in the H<sub>2</sub> evolution was then evaluated, using either UV or solar light as irradiation sources and biomass-derived alcohols such as ethanol or glycerol as sacrificial donors. As expected, in the case of UV irradiation, the activity was much higher. Activity in the photoreforming of ethanol were remarkable, on par with benchmark carbon-supported catalysts, with rates as high as 25

mmol g<sup>-1</sup> h<sup>-1</sup> with the catalyst with 20 wt% MWCNTs. The fact that the material with more CNTs gives better activity suggest the key role of the carbon nanostructure. Both compositions were however much higher than the corresponding CNT-free catalyst. As expected, when using glycerol as sacrificial agent, activity was substantially lower, in agreement with literature findings, reaching however good rate of H<sub>2</sub> evolution. Obviously, when simulated solar light was used, activity dropped. In any case, the H<sub>2</sub> production was higher than most state-of-the-art catalyst, considering the use of Pd instead of the typically employed Pt and the lower lamp power utilized as compared to most studies.

The same materials were also tested in the electrocatalytic H<sub>2</sub> evolution, arising from H<sub>2</sub>O reduction. This is an important alternative as no sacrificial agent needs to be added in the reaction mixture. A GCE electrode modified with various catalysts, including reference catalysts such as CNTs/Pd and Pd@TiO<sub>2</sub>, was assembled by drop casting dispersions of the catalysts. The activity toward the H<sub>2</sub> evolution at neutral pH was outstanding, with turn-over frequencies (TOFs) in excess of 141.000 h<sup>-1</sup> and applied overpotentials as low as 40 mV when using the calcined catalyst MWCNTs/Pd@TiO<sub>2</sub>. The mechanism proposed is based on electrochemical investigation, and features Pd as the truly active site. However, a comparison with MWCNT-free catalysts (Pd@TiO<sub>2</sub>) or TiO<sub>2</sub>-free catalysts displays that the other two phases are also necessary, in particular the MWCNTs favors electron transfer processes, while TiO<sub>2</sub> serves to initiate the dissociative activation of the water molecule at neutral pH. On the other hand, physical mixtures of MWCNTs and Pd@TiO<sub>2</sub> displays lower performance, and this fact highlights the enormous importance of the maximized contact of MWCNTs and inorganic matrix

Next to carbon nanotubes also other carbon nanostructures were used, namely carbon nanocones (CNCs) (Figure 14). These CNCs have better dispersibility compared to CNT, resulting in structures with a higher degree of homogeneity.

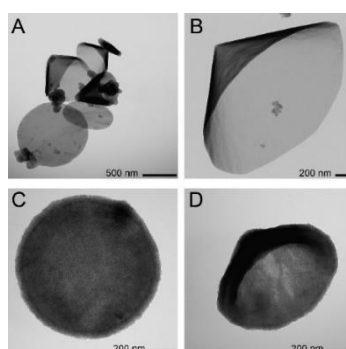


**Figure 14.** Representative TEM images of ox-CNCs with cones and disk-like morphology (A and B) and ox-CNCs/Pd@TiO<sub>2</sub> in both disk-like (C) and conical (D) morphologies;

These CNC catalysts were then tested in the H<sub>2</sub> evolution using ethanol as sacrificial donor under UV or simulated solar light, and activity are reported normalized by the surface area, in view of the considerations made above for the nanotube analogues. Strikingly, activities were significantly higher (about 30%) than those found for the CNTs, reaching a H<sub>2</sub> production rate as high as 37 mmol g<sup>-1</sup> h<sup>-1</sup> under UV irradiation.

As a last material for energy application, a new metal-free catalyst comprising carbon nanohorns (CNHs) enveloped in a shell of N-doped graphitic carbon were designed and prepared (figure 15). N-doped carbon has been reported in literature as an effective catalyst for the electrocatalytic O<sub>2</sub> reduction, a half-reaction occurring at the cathode in certain types of fuels cells. The electrocatalytic activity toward the reduction of O<sub>2</sub> was therefore evaluated, and it was interesting to note that in contrast with most of the reported systems, the present catalyst could selectively drive the formation of H<sub>2</sub>O<sub>2</sub> (the 2-electron reduction product) instead of water (the 4-electron reduction product). This

has an extra advantage, as hydrogen peroxide is a ubiquitous molecule in industry, employed in many sectors.

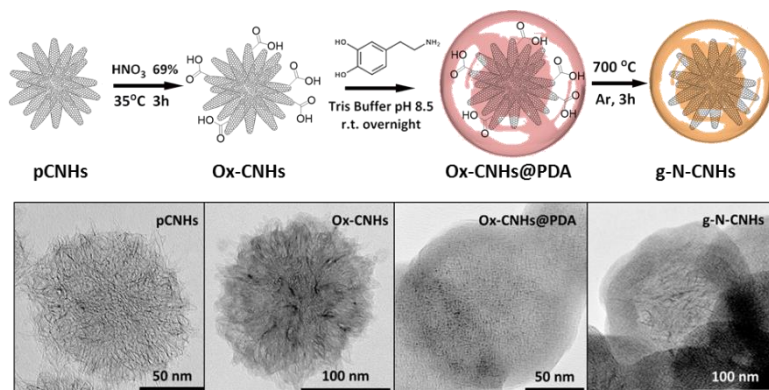


**Figure 15.** Top: Scheme of the synthetic protocol to obtain g-N-CNHS. Bottom: TEM images of the nanostructured material at each stage of the synthesis

The findings of this specific work related to WP3 are very important as they combine the development of a cathodic material for fuel cell application with the efficient and sustainable production of an industrially crucial molecule, without using any metal-based catalyst.

In a final part, Eu(III) complexes were successfully encapsulated inside CNTs, by designing and synthesizing a C60-appended ionic liquid nano-carrier (Figure 16). This approach allowed us not only to increase the filling ratio within thinner tubes, namely single and double-walled CNTs, but also to control the organization of the chromophores within the tubular framework. Photophysical investigations showed that the entrapment in different CNTs causes a different degree of emission quenching. The luminescent materials have been injected in cells, and their emission detected by confocal imaging (Figure 17).

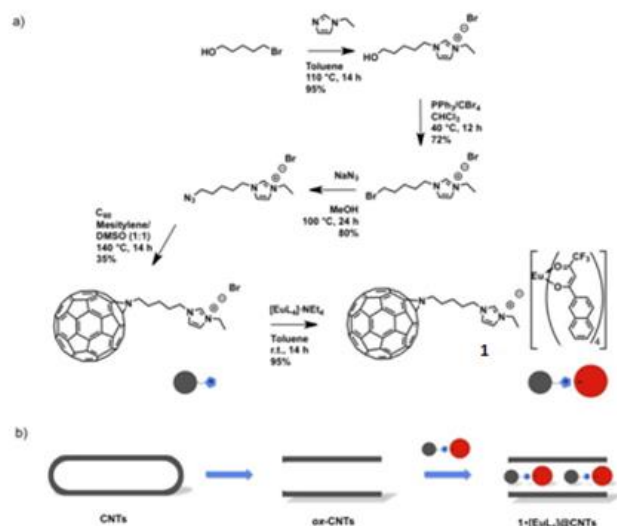


**Figure 16.** a) Synthetic procedure adopted for the preparation of the supramolecular complex **1**; b) Schematic representation of the filling approach for encapsulating ion-paired complexes.

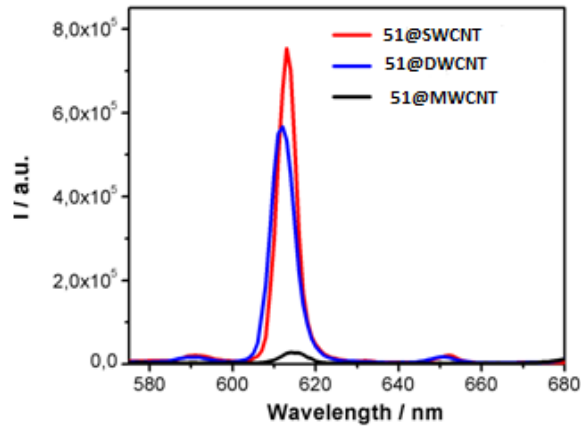


**Figure 17.** Emission profiles ( $\lambda_{exc} = 375 \text{ nm}$ ) of KBr pellets (1 mg of encapsulated material mixed with 10 mg of KBr) containing **1@SWCNTs** (red trace), **1@DWCNTs** (blue trace), and **1@MWCNTs** (black trace).

#### WP4

The most promising phosphors developed in this project, in terms of luminescence performance and chemical stability, were selected to fabricate a suspension containing Ag-zeolite phosphors. This formulation was used in the coating of glass tubes that subsequently were converted into fluorescent lamps. Preliminary results showed that the coating of the fluorescent lamps with Ag-zeolite phosphors is feasible, as a working lamp was obtained. However, certain problems associated with the agglomeration of zeolite particles were observed and lifetime and yield of the lamp did not yet fully meet the standards required for commercial lamps (Figure 18).

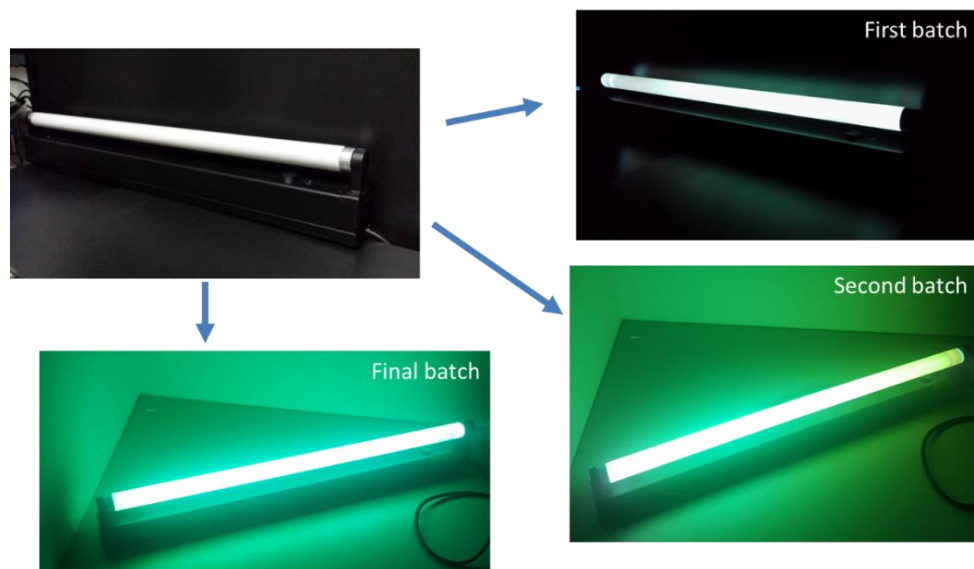


**Figure 18.** different batches of SACS phosphor containing prototype fluorescent lamps.

Full optimization directed to the creation of Ag-zeolite phosphors to be utilized in the fabrication of fluorescent lamps is ongoing in collaboration between Leuven and Philips R&D, with the second lamp model already showing improvement. Further additional improvements in quantum yield and stability of the phosphors, led to development of the third generation of lamps showing again an improvement of lamp quality, however further research for complete optimization is still ongoing.

Apart from the fluorescent lamps, great opportunities lie in the development of LED materials. As has highlighted by the industrial partner, Philips, this is specifically the case for red emitting hybrid materials. Hence, current development work within the SACS project is using the new phosphors for LED application, with new prototype demonstrators based on UV LEDs as UV source (Figure 19).

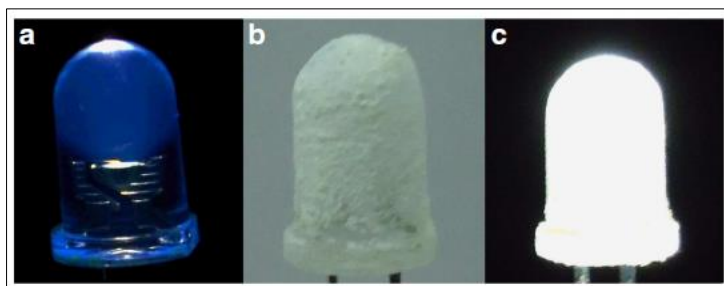


**Figure 19.** Examples of LED prototypes prepared by dipping a UV emitting LED in a phosphor, resulting in white light emission.

However during the SACS project, different other potential applications of these metal zeolites were discovered, which will be further investigated and optimized.

Some of these other potential applications besides to their use as phosphor are depicted in Figure 20, such as smart fluorescent labels, luminescence based sensors and catalytic bodies.

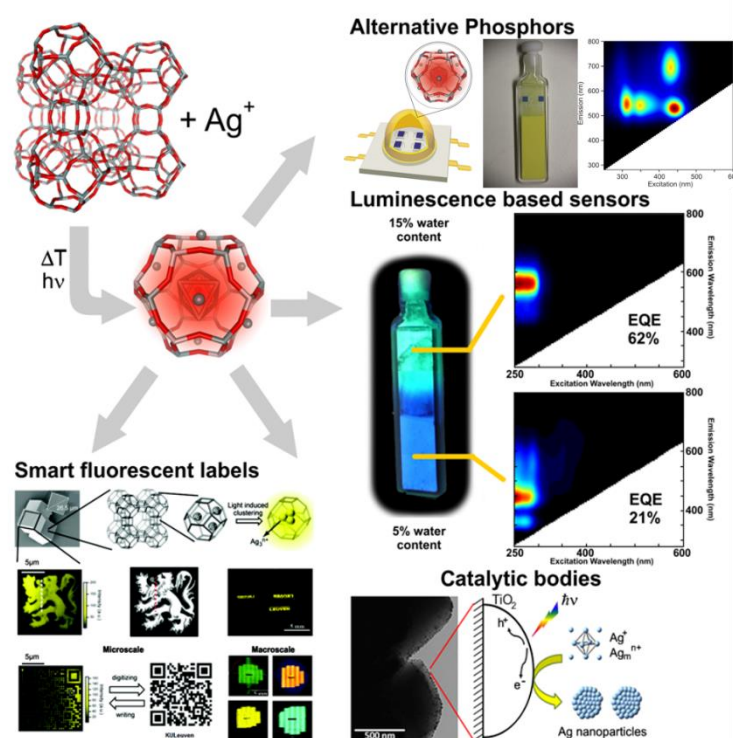


**Fig 20.** potential applications for silver and other metal zeolite composites.

Additional efforts were investigated in researching the electroluminescent properties of the most interesting MOF sample presented in the SACS project; namely the (silver-loaded) bio-MOF-1 and related samples. For their use in OLEDs, which probe the electroluminescence of the metal-organic frameworks (as organic emitter in pane) (Figure 21).



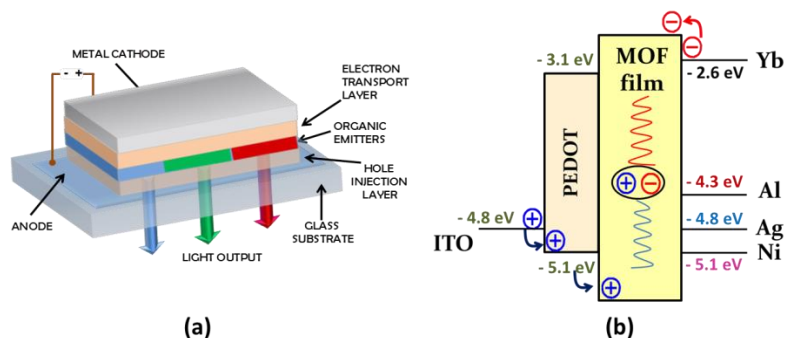


**Figure 21.** Schematic (a) and energetic (b) representation of the OLED setup.

From the electrochromic materials synthesized in this project have been successfully tested in electrochromic devices (ECD). Through a collaboration of between FFCT-UNL, UniSTRA, UCardiff and Yvisible several hybrid materials were successfully tested in ECDs, yielding a range of colours, at varying performances.

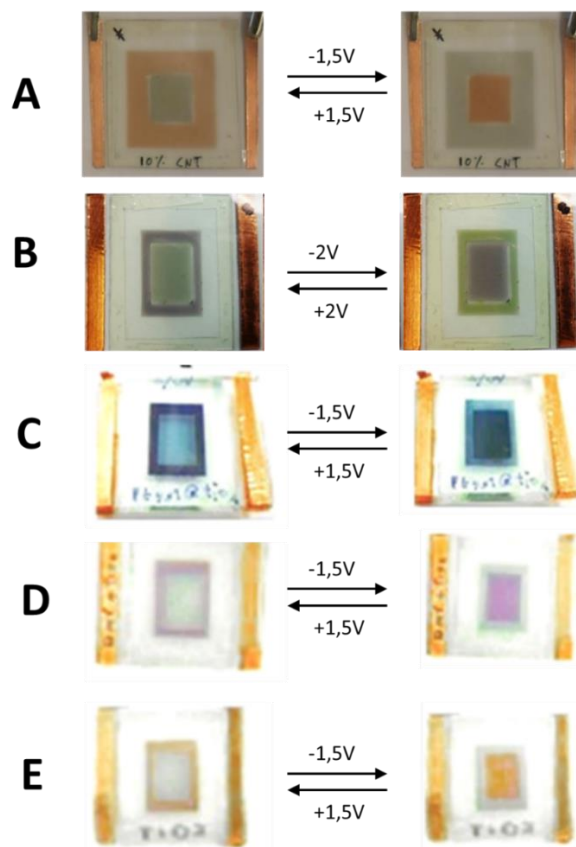


**Figure 22.** - Pictures of ECD based on the hybrid electrochromic materials successfully tested and characterized in solid-state devices. The inner square of the device patterns is the working-electrode. The working-electrode of the devices on the left column are in their oxidized form, i.e. bleached state and on the right column in their reduced form, i.e. colored state.

#### Performance testing

The performance of the different TiO<sub>2</sub> based hybrid materials is in general better when these synthesized using electrochemical polymerization of the polythiophene on to a TiO<sub>2</sub> template layer

coated on the surface of the ITO electrode (for experimental details on the synthesis strategies please consult WP2 report). However, the PDMT/TiO<sub>2</sub> obtained by sublimation had the best coloration efficiency (386 C<sup>-1</sup>cm<sup>2</sup>).


The space confinement of the polythiophenes in the TiO<sub>2</sub> mesoporous structure resulted in a bathochromic shift of the maximum absorption wavelength peak of the PEDOT/TiO<sub>2</sub> (obtained by sublimation) based devices. Pristine PEDOT presents a deep blue color, while the respective hybrid material in TiO<sub>2</sub> presents a purple color. This mechanism could be used to develop and/or fine-tune electrochromic colors by spatial confinement:

Finally, it was found that the size of the TiO<sub>2</sub> mesoporous nanoparticles had a dramatic impact on the switching times of the display. The PEDOT and PDMT electrochromic polymers were encapsulated in different TiO<sub>2</sub> mesoporous materials with different particle size: a) >μm and b) 600nm. Both hybrid materials with the smaller TiO<sub>2</sub> particle size presented faster switching:

#### *Lifetime testing*

The lifetime testing of the above described devices were satisfactory (Currently classified information, see more detailed information in D4.2.2 report). All the devices succeed to be reversibly cycled with satisfactory color contrast for several thousands of cycles. The best result found was for the SACS hybrid materials that showed an improved durability when compared to its pristine polythiophene material. All the devices characterized in WP4 classified for the accelerated aging test. In which the devices were cycled repeatedly using a square-wave voltage function in some cases between -1.5V and +1.5V and in other cases between -2V and +2V. The color contrast as already mentioned was monitored using a CCD camera at different cycling periods. The results of these test are shown in table 4

**Table 4.** Life-time results of accelerated cycling tests on the hybrid based ECDs. Results show the minimum number of cycles performed in the devices until 50% of the initial colour contrast is lost. Structural description of SACS material is blocked for IP reasons.

Hybrid EC material	Number of cycles performed to reach lose 50% of the initial color contrast
	>40000
PEDOT/TiO <sub>2</sub>	>200 <sup>#</sup>
PDMT/TiO <sub>2</sub>	>2000
PEDOT/TiO <sub>2</sub> *	>10000
PDMT/TiO <sub>2</sub> *	>40000
P3MT/TiO <sub>2</sub> *	>1000

<sup>#</sup>Due to technical issues the cycling test was only monitored in the first 200 cycles

In the final part the catalyst materials which were developed throughout the SACS project were benchmarked and up scaled to larger pilot reactors. Furthermore the developed catalyst were tested for there recyclability

#### *1) Catalyst for hydrogenation based on Ag nanoparticles*

The selectivities of the chemoselective hydrogenation of cinnamaldehyde by commercial AgNO<sub>3</sub>/SiO<sub>2</sub> (10 wt%) (Sigma-Aldrich-248762) is along the same line as observed in the smaller reactors. However, the reaction occurs much slower in the large 100 mL reactor (58% conversion after 6 hours, Table 2, entry 1) compared to the attained 90% CALD conversion (Table 1, entry 5) after 4 hours in the smaller 10 mL reactor. This observation of slower reaction holds even more for the Ag/UiO-66 catalyst at the



larger scale. It shows that the reaction occurs a lot slower on the large scale (2% conversion after 6 hours), compared to the small reactor (82% conversion after 6 hours). Even more, the selectivities have drastically shifted drastically, where the selectivity towards the desired CALH has dropped to 58%, while 18% of the fully hydrogenated, undesired HCALH is produced. This result is more in the line of, but not as bad as the Ag/Al<sub>2</sub>O<sub>3</sub> catalyst in the small reactor.

Possible explanation for this (s)lower catalytic activity and worse selectivity in the large reactor are the different mass and heat transport phenomena at this larger scale. Another, explanation is the different headspace volume and accompanying hydrogen gas dissolution in the solvent compared to the reactions in the small reactor. Additionally, the upscaling of the silver-loading could have been another problem point, as the loading could have occurred less homogeneously and/or less efficiently compared to the small scale

While the preliminary results on the chemoselective Ag-catalysed hydrogenation of cinnamaldehyde in small reactors prove to be satisfying, further research is needed on the different effects during upscaling of the silver-loading and of the catalytic reactions in larger reactors, moving towards pilot-scale and industrial applications.

## 2) MWCNTs/Pd@TiO<sub>2</sub>

Carrying out several syntheses in parallel, each generating 300 mg of product and combined all the product. We obtained approximately 1 g of hybrid of good quality, which was used for a 1 g test in the photoreforming of ethanol. Typically, on a lab test scale, we had used 10 mg of catalyst dispersed in 60 mL of EtOH/H<sub>2</sub>O mixture, which is also the maximum capacity of the UV photoreactor. Passing to 1 g of catalyst implies use of a 100 time more concentrated dispersion of the catalyst, which is therefore not as homogeneously dispersed. This caused a significant drop of activity in the H<sub>2</sub> evolution if expressed by the gram of catalyst, going from 27 mmol g<sup>-1</sup> h<sup>-1</sup> to 8 mmol g<sup>-1</sup> h<sup>-1</sup> of evolved H<sub>2</sub>. The quantum efficiency also drops from 21% to 2%.

The results obtained strongly suggest that an upscaling of the materials must necessarily rely on labs appropriately equipped, given that the synthetic protocol critically depends on factors such as concentration of the MWCNTs building blocks. This can be circumvented by successive syntheses, which is however very time consuming. The catalytic tests also require use of appropriate photoreactor. Industrial labs must be involved for a better evaluation of the catalyst on large scale set-ups.

## *Recycling protocols for materials based on Fe@MWCNTs*

### *Magnetic filtration*

Firstly, the four different Fe@CNTs were tested in their ability to be magnetically removed from a solution. Typically, the four kinds of Fe@CNTs-NHCO-Ab have been dispersed, at a constant iron concentration, with a tip-sonicator and immediately placed at 3 cm of a strong permanent Ne-B magnet for different amounts of time (30 sec, 120 sec and 480 sec). The ratio between the absorbance of the removed supernatant vs the absorbance of the re-suspended magnetically generated precipitate gave us the proportion of non-coagulated CNTs. No dramatic differences in the coagulation profiles were found between the different kinds of Fe@CNTs. However, one can see that HCl-Fe@CNTs seem to be the best candidates in terms of speed of coagulation and lowest final amount remaining in solution (“coagulation effectiveness”), i.e. 20% versus 27% for Fe@CNTs and ann-Fe@CNTs and 22% for ref-Fe@CNTs.

$$\text{Coagulation effectiveness at time } t \text{ (\%)} = \left(1 - \frac{(\text{Absorbance}(t) - \text{Absorbance blank})}{\text{Absorbance}(t=0)}\right) * 100$$

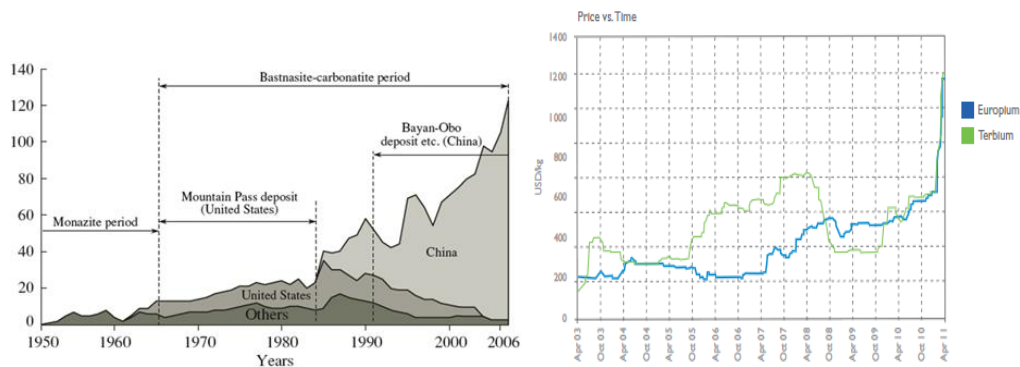
## Potential impact and the main dissemination activities and exploitations of results (10P)

The SACS project targeted the generation of highly performing materials via self-assembly of nano-scale building blocks at industrially relevant scales for use in nanotechnology based consumer goods.

Among the key applications envisioned in the original project are:

- 1) Small metal clusters luminescent clusters for use in lighting and catalysis applications
- 2) Nanostructured assemblies of dyes in porous materials, for use as emissive materials, in electrochromic devices
- 3) Functional carbon nanomaterials for use in energy related applications and catalysis

In this first key application, the SACS materials target a market for fluorescent lamps and LED lightings which is estimated to account for a revenue of € 20 billion in 2015 and observing rapid growth, reaching € 100 billion in 2020. Major drivers for these market trends are an increasing ban on energy inefficient lighting combined with demographic changes, with 70% of people living in a city in 2020. At the same time global changes in the availability of Rare Earth Oxides, the key luminescent components of these lamps, place pressure on the demands and prices. A notable example, are the 2011 price spikes, with the price of Rare Earth Oxides fluctuating between 300% and 2500% over a period of 8 months.



This results in a quest for alternative sources to fulfill the current demand and depend less on the global market supply, a quest of which the SACS project is part. SACS synthetic phosphors/emissive materials may create an important economic impact in the lighting industry by being an independent source of phosphors for the European market, reducing the amount of phosphor material utilized per lamp unit as well as the production costs on a larger scale.

So far, economically viable alternatives for the rare-earth phosphor materials do not exist. Currently, only rare-earth based phosphors are used as phosphors in lighting applications (Yen 2007), since these are the only commercially viable materials that are sufficiently photostable upon UV or blue excitation and that meet all the industrial requirements. These materials have light conversion efficiencies of 80 to 95%, being the result of over 40 years of phosphor optimization.

In general luminescent materials can be divided in several classes, of which the rare-earth phosphors, the traditional organic fluorophores and the semi-conductor-based quantum dots are the most important. The organic fluorophores are immediately excluded for consideration as replacement for

rare-earths in lighting devices due to their very limited photostability and small Stokes shift (defined as the energy difference between the maxima in absorption and emission spectra).

As such, the main advantages of these new luminescent materials can be summarized as follows:

- Increased photo- and chemostability due to the confinement in the porous host, excluding e.g. oxygen and other oxidizing species.
- Spectrally broad emission bands (in contrast to rare earths), providing a higher color rendering index for the emitted light
- High tunability of the spectral characteristics of the emissive materials, to meet the specific requirements of the different lighting applications
- Cheaper raw materials
- Wide availability and less toxicity of the raw materials, making the market less dependent from the Far-East for material supply.

All the SACS phosphors developed in the project are synthetically fabricated from abundant raw materials. Additionally, zeolite production is widely available worldwide not being in a monopoly situation. The excellent research results and development already achieved in the fabrication of SACS phosphors/emissive materials let us believe that high quantum yield materials with values above 90% can be reached. This will have a strong impact on the lamp light quality and on the required amount of phosphor in the fluorescent lamp coating. The result will not only lead to cost reductions but also to an environmental impact due to the potential recyclability of the exhausted materials.

Based on a conservative cost estimation, the bill-of-materials (BOM) of the developed SACS Ag-zeolite material has been projected around 52€/Kg. This places the current SACS phosphors in the range of commercial of natural REO triband phosphors (~60 €/Kg).

Within the project, a large number of luminescent materials were thoroughly characterized and evaluated for their physical parameters, such as quantum efficiency, chemical stability and spectral properties. Through structure-activity relationships, these were optimized for use in lighting application.

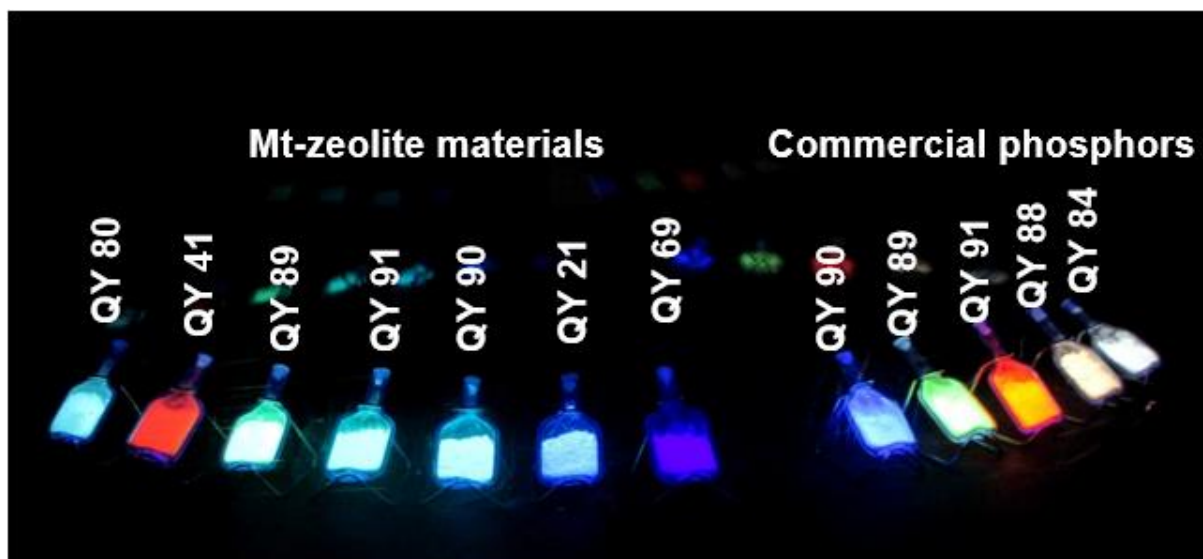


Figure 1. Fluorescent phosphors of the SACS portfolio compared to their industry counterparts

The most promising Ag-zeolite phosphors, in terms of luminescence performance and chemical stability, were selected to fabricate a suspension containing Ag-zeolite phosphors. This formulation was used in the coating of glass tubes that subsequently were **converted into fluorescent lamps**.

In the final batch an atomic layer deposition (ALD) coated green SACS phosphor was used, to prevent hydration between deposition and lamp fabrication. Furthermore the phosphor aggregation was prevented by sieving the phosphor suspension prior deposition, by this way it was possible to remove large aggregates, which will eventually lead to the brown coloration. Sieving was performed using a vibrating sieve.

These lamps resulted in a more homogeneous green emitting lamp (Figure 4.1.20). For these lamps the coating is much more homogeneous and no brown aggregates are observed (Figure 4.1.21).



Figure 2 Third batch of FL prototypes using optimized SACS phosphors.

Over the course of the project, **the lighting market has entered a phase of profound changes**. Due to increasing regulation, the shift of energy inefficient fluorescent lighting to LED lighting has achieved momentum. This poses significant challenges for the SACS phosphors, as major lamp manufacturers reduce R&D investments in these depreciated technologies or restructure their existing lamp entities. This was not only evidenced by the structural changes at one of the SACS industrial partners Philips, splitting its lighting division, but also for example the recent intent to close the European lamp

production by Sylvania. Hence, these market challenges have prompted the consortium to **investigate the use of the SACS phosphors for LED use.**

While fluorescent lamps are nowadays being replaced by LEDs at an increasing pace, the current LED phosphors are also Rare Earth containing materials which are additionally, due to patent regulations, reaching prices of 10.000 to 20000 \$ /kg. Hence, the SACS consortium started focusing on the synthesis of metal zeolite-based LED phosphors: these phosphors should be blue or near-UV excitable, have high EQE and preferentially emit broad white light.

In this light it is also noteworthy that in a collaboration between the SACS partners, a new type of Zeolite phosphor has been developed, and these phosphors have very broad white emission which is tunable to more cool bluish and warmer white light and reach quantum yields up to 40%. At this very moment, further optimization and structure characterization of these new and exciting type of materials is ongoing.

In addition to their lighting use, the SACS consortium has uncovered diverse other applications for its materials. They are currently under investigation for use as sensors which have a simple and clear colorimetric readout or as smart label (see image below). Through these additional applications, the SACS consortium seeks to uncover additional markets.

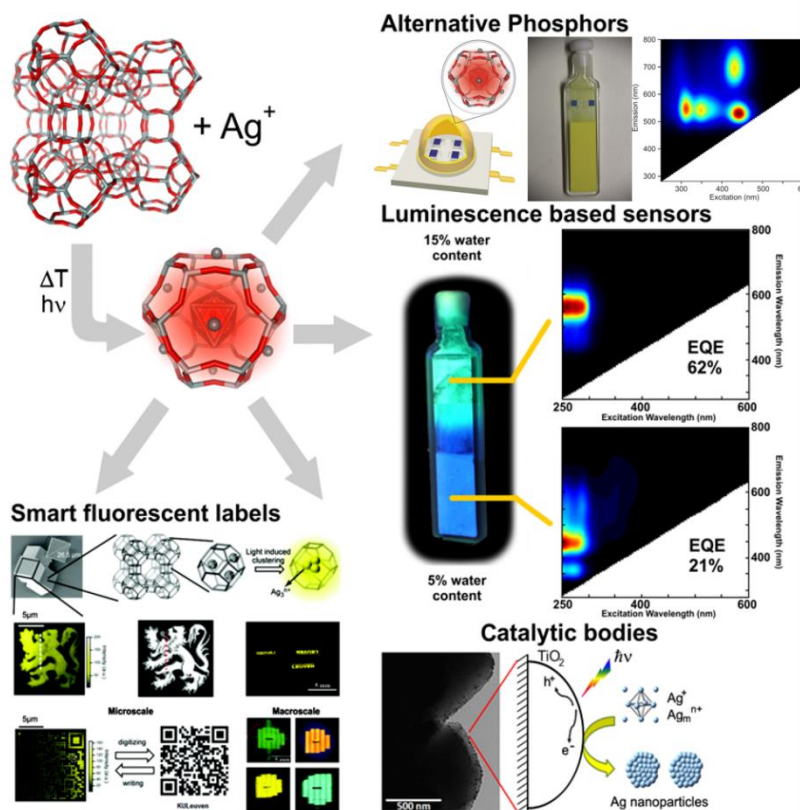
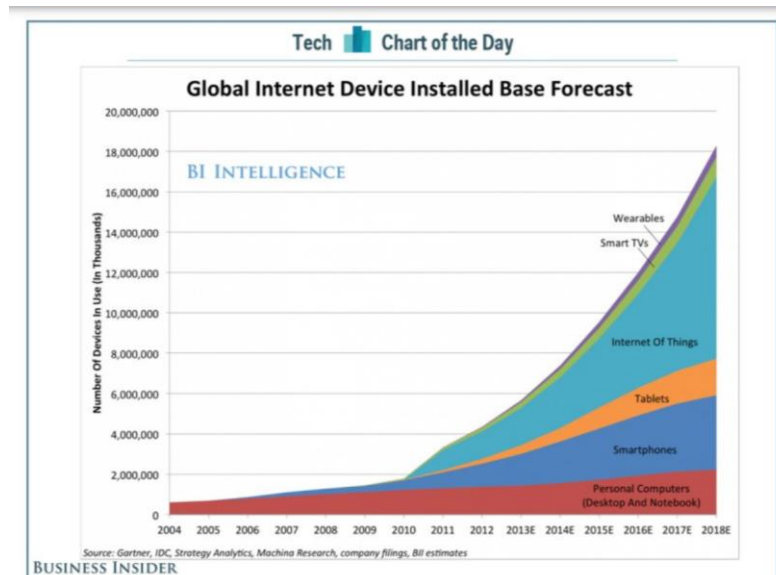


Figure 3 Additional applications for the SACS materials uncovered in the project

For the second key application, the SACS consortium has developed novel materials **for electrochromic devices**. Such devices will be one of the key enabling technology components that form an integral part of the “internet of things”, the collection of over 50 billion connected devices collecting and analyzing information. On the interface of this internet of things and the real world, there is a need for energy efficient ways of visualizing all its information, leading to the predicted installment of several hundreds of millions of electrochromic devices. Give the vast impact on human society, this market is estimated to reach no less than 660 Bn UDS by 2021.



Today, electrochromic technology (ECT) have found real applications in different markets like automotive and in energy saving architecture (Smart Windows). The potential economic impact resulting from an improvement of the state-of-the-art in electrochromics can be measured by: a) increase of the competitive advantages against competitive technologies like e-ink or liquid crystal; b) new features that will allow its application in new markets and c) development of new products.

The two main markets where ECT is having considerable success are smart windows and automotive (darkening rear-view mirrors). The improvement of the state-of-the-art of ECT will strengthen its market position face to other competitive technologies. It is estimated that Smart Windows market will reach about US\$6Bn in 2020. Additionally the Global Auto-dimming Mirror market is expected to be worth more than US\$3 billion by end of 2016.

These trends required the development of inexpensive and durable materials that can easily be printed and have low energy consumption. Within the SACS project, electrochromic devices (ECD) using hybrid materials were successfully developed and tested. Initial characterizations tests showed the importance of the hybrid synthesis procedure and the resulting electrochromic functionality. ECD with the hybrid material obtained via ship-in-a-bottle in liquid state were functional and even **presented an improved durability when compared with the pristine chemically polymerized PEDOT devices**.

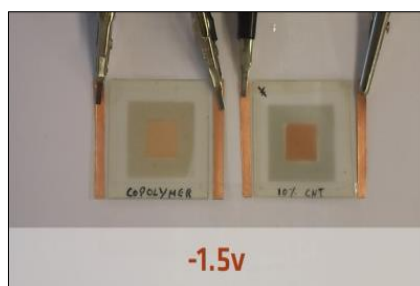


Figure 4 Electrochromic prototypes prepared to study the SACS materials.

Additional electrochromic devices were assembled with other SACS hybrid materials-blends, which led to enhance the ECD performance when compared to devices assembled with pristine pyrene-appended PEDOT electrochromic material. The new materials display increased switch speed, with the new devices up to **12 times faster**, consuming **38% less energy**, whereas the total transmittance modulation is ca. 37% higher and the **cycling stability is improved** in one order of magnitude. This **key result has great commercial significance, and is part of an ongoing patent application** and evaluation for commercial use.

As such SACS uncovered materials that may be deposited in the usual industrial methods (spray-casting, screen-printing). Such materials enable the development of new colours, allows the fine tuning of the color and the reversibility of the device i.e., by playing with the supramolecular structure. Since electrochromes are within the conductive layer architecture, we also expect enhancement of switching times and coloration efficiencies.

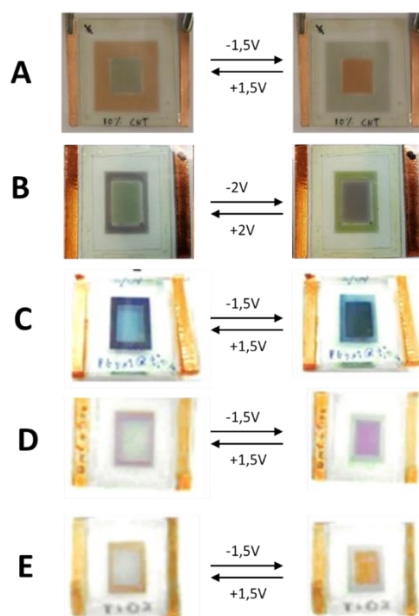


Figure 5. Colour portfolio of the SACS materials

Task 2.2 delivered two different protocols for the synthesis of electrochromic materials. In the first protocol we followed electrodeposition techniques, in which the electrode is modified previously, in order to generate mesoporous thin-films in which an electrochromic polymer was then synthesized in the confined space. This strategy led to prototypes at WP4 with high cyclability. This result from the scientific point-of-view was important as proof-of-concept, but has the drawback of non-reproducible protocols, to be implemented in commercial available procedures. That was why a second protocol



was delivered in which the electrochromic polymer is synthesized directly in mesoporous TiO<sub>2</sub> nanoparticle powders developed by P4. Now we have a material that can be deposited by conventional industrial methods (spray-casting, screen-printing). Such materials enable the development of new colours, and it is identified as an Exploitable Result (ER-1).

Electrochromic devices (ECD) like the ones developed in SACS project have used ITO based electrodes, Indium Tin Oxide, or ITO, is a key material for current electronics and displays as is a transparent and conductive material. The transparency allied with the electrical conductivity make this material the number one choice for the production of transparent electrodes used in the large majority of display technologies, like LCDs and OLEDs. Alternative display technologies like electrophoretic displays (E-Ink), and new products based on photovoltaics also use ITO as transparent electrode.

At the ECD component level, the key material cost element is that of ITO (3 Bn \$ in 2010 with a 20% growth rate through 2013) Moreover, ITO suffers from several drawbacks: (i) indium is becoming a scarce and expensive resource; (ii) it exhibits serious technical issues (deposition techniques are expensive, quite inefficient and slow; ITO films are fragile, sensitive to corrosion and have a relatively high index of refraction. As ITO is growing increasingly scarce and expensive, the search for alternatives is on.

Over the course of the SACS project, novel and promising alternatives for the ITO film have been developed, by applying the core SACS concept. As such, we are not only forwarding the core electrochromic components used in ECD devices, but also the materials used in electrode preparation for such devices (example of device shown below).

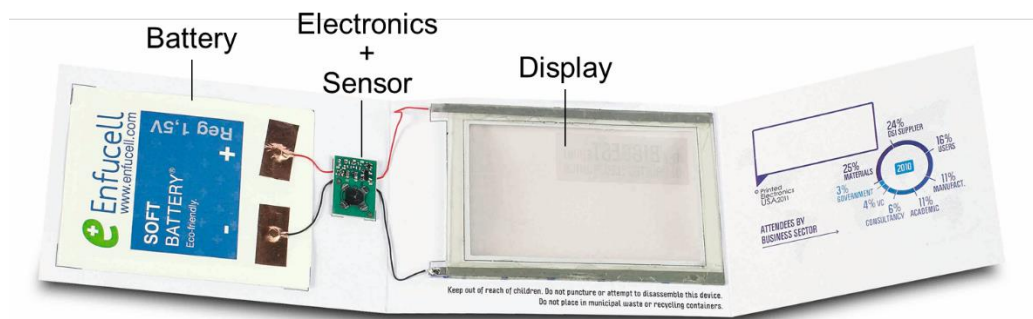


Figure 6 Ynvisible's Interactive Badge produced for IdTechEx

In its **third objective**, the SACS project aimed for catalytic applications of the nano-assembled materials. Here, the main targets are cleantech related, involving hydrogen and CO<sub>2</sub> conversion. Carbon dioxide capture and conversion fits in the fight against global warming and green-house gasses, and is of the ultimate importance to society. With hydrogen conversion reactions, such as the water-gas shift reaction, we target the \$100 Billion H<sub>2</sub> production market, and hydrogen fuel cell vehicles are one of the top 10 emerging technologies of 2015. As such, the momentum is high for these alternative sources of energy.

Catalysis is universally recognized as a key enabling technology for greening the chemical industry and for efficient energy conversion. No matter what the energy source is – oil, natural gas, coal, biomass or solar – a clean sustainable energy future Apart from improving the performance of existing industrial processes for energy production, nano-catalysts have the potential to lead to exploitation of



renewable, efficient, and inexpensive sources for alternative energy production. Rationally designed Nanocatalysts, as have been developed by the SACS consortium, also have the potential to reduce Europe's reliance on imported rare earths/precious metals, which form the bulk of current industry catalysts. Furthermore the nanostructured photoactive systems proposed have a strong potential in pushing photocatalysis towards industrial relevance. One very direct application of the SACS catalysts will be in providing high purity hydrogen for fuel cells, by minimizing the concentration of the CO poison via WGS or PROX reactions. Uniquely stable and efficient catalysts will become available through the SACS approach. As a second testing case for the composite metal catalysts based on CNTs, we will study the electro-oxidation of ethanol for use in direct alcohol fuel cells. Fuel cells are an integral part of clean energy technologies. While versions based on anodic H<sub>2</sub> or MeOH oxidation are fairly well established, there is a need for fuel cells that can directly use ethanol. Ethanol will be massively available in the near future from biomass feedstocks, either originating from agriculture (first generation bioethanol) or from forestry and urban residues (second generation bioethanol). Additionally, ethanol use opens options to decrease the cost of the membrane electrode assemblies, which will give a boost to the commercialization of direct alcohol fuel cells.

To this purpose, several metal-carbon hybrid catalysts were successfully tested and characterized, to varying degrees of success. For example, the Fe@MWCNTs/Pd@TiO<sub>2</sub> presented a catalytic activity for the photoreforming process of 9 mmol(H<sub>2</sub>)·gcat<sup>-1</sup>·h<sup>-1</sup>, **which makes the SACS catalyst much more active than the typical benchmark catalyst** Degussa P25. A laboratory scale demonstrator was successfully developed where hydrogen production from a mixture of water-ethanol can be observed. Initial efforts for the scale up of the SACS catalyst preparation have been undertaken within the project, and industrial collaboration with industrial partners for both production and performance evaluation have been struck.

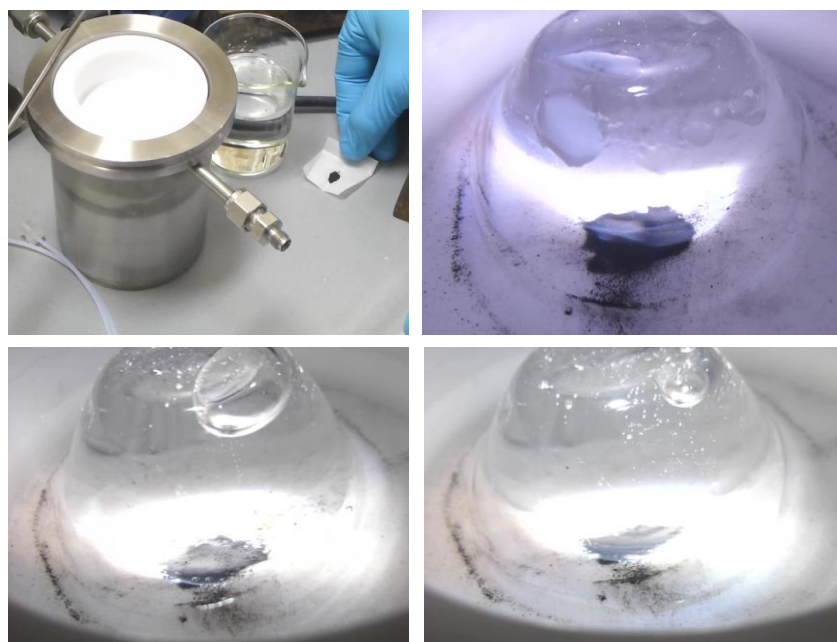


*Figure 7. Laboratory scale light induced hydrogen production*

Over the course of the project, several new opportunities have been identified that lie outside of the exploitable results as defined in the ESS seminar, but are pursued nonetheless. Amongst these results are diverse subjects such as biological imaging with silver nanoparticles (P2), cancer cell death using

Fe@MWCNTs in Magnetic Fluid Hyperthermia (P5), mercury sensing with luminescent phosphors (P1) photoluminescent pigments with quantum yield equal to 52% (maximum emission at 650 nm) (P3) as a side product which might be exploited as well.

### **Scientific publications**

The scientific knowledge and technology insights generated within the SACS project have been the subject of a proliferative publication pipeline. Over the course of the project, the SACS consortium has published results in such top tier journals as Nature Materials, Small, Advanced materials and Nature, leading to 47 distinct publications. In addition, the scientific results have been the topic of no less than 127 posters and scientific lectures, at scientific conferences across the globe.

In a final workshop, dedicated to the scientific concepts of Self-Assembly in Confined Space (SACS), September 2016, San Sebastian, Spain the project main results were presented to a global audience.

### **Further Development and Exploitation of the SACS materials**

The SACS consortium commits to further seek exploitation of the key results with prototype devices and demonstrators which could lead to novel products, through further R&D based on the newly gained insights, and in collaboration with industrial partners.

## **Address of the project public website**

Website: <http://www.fp7-sacs.com>

## **SACS Coordinator:**

Prof. Dr. Johan Hofkens, KULeuven, Belgium

Johan.Hofkens@kuleuven.be